

High bandwidth waveguide photodetector based on an amplifier layer stack on an active-passive semi-insulating InP at 1.55 μm

M. Nikoufard, L. Xu, X.J.M Leijtens, T. de Vries, E. Smalbrugge, R. Nötzel, Y.S. Oei, M.K. Smit

COBRA Research Institute, Technische Universiteit Eindhoven
Postbus 513, 5600 MB Eindhoven, The Netherlands

A waveguide photodetector based on semi-insulating indium phosphide (InP) was designed and fabricated. The layer stack for this photodetector was optimized for use as an optical amplifier or laser. By reversely biasing the structure, an efficient, high-speed photodetector was made, which allows for easy integration of source, detector and passive optical components on a single chip. Based on the simulation results, we designed a $30\ \mu\text{m} \times 1.5\ \mu\text{m}$ waveguide photodetector integrated with a passive access waveguide, which has achieved a 3 dB bandwidth of 35 GHz and 0.25 A/W external responsivity at 1.55 μm wavelength at $-4\ \text{V}$ bias voltage.

Introduction

The photodetector is a key component in the optical communication system[1]. One of the requirements on photodetectors is a high bandwidth-efficiency product. Compared to the top-illuminated photodetector, the waveguide photodetector has the advantage of almost independent relationship between the bandwidth and the efficiency[2]. Although it has a disadvantage in the fiber-chip coupling efficiency, it is easier to be integrated with laser/preamplifier, AWGs, and other passive components. By optimizing the waveguide geometry and absorption layer thickness of the waveguide photodetector, high bandwidth-efficiency product of 55 GHz has been reported[3]. However, the layer stacks of these reported devices are not suitable for the realisation of semiconductor optical amplifiers (SOA) or lasers, which would limit the flexibility in the monolithic integration of the source and the detector. In[1], the laser is based on quantum wells while the photodetector is based on bulk material, and 12.5 Gbit/s per channel is achieved. To ease the technology for such an active-passive integration, we investigate RF bandwidth of the photodetector by using the same layer stack as SOA/laser. For proper RF performance, we use a semi-insulating InP substrate and coplanar waveguide design. The measurement results show that a $30\ \mu\text{m}$ ($80\ \mu\text{m}$) long photodetector can operate up to 35 GHz (28 GHz) with external responsivity up to 0.25 A/W (0.35 A/W) at a wavelength of 1.55 μm .

Design and Fabrication

The layer stack shown in figure 1 which was previously used for fabricating lasers and optical amplifiers[4], is now being used for the realization of high-speed photodetectors. Due to n.i.d. doping in the film layer, this film layer will be completely depleted even under a small reverse bias voltage. Therefore, in the following calculation, the depletion

300 nm InGaAs $p=1.5e19$ max	
1000 nm p-InP $p=1e18$	
300 nm p-InP $p=5e17$	
200 nm p-InP $p=3e17$	200 nm n-InP $n=6e16$
190 nm n.i.d Q1.25	360nm n-Q1.25 $n=6e16$
120 nm i-Q1.55	
190 nm n.i.d Q1.25	
200 nm n-InP $n=5e17$	
900 nm n-InP $n=1e18$	
SI-InP	

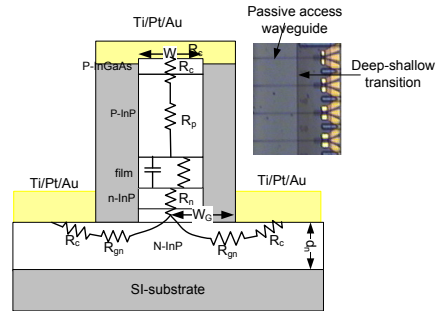


Figure 1: Active-passive butt-joint layer-stack with specifications based on a semi-insulating substrate .

Figure 2: Schematic of the crosssection and a photograph of finished devices.

layer thickness was taken as 500 nm, the same as the thickness of the film, corresponding to a 44 GHz transit time bandwidth[5, 6]. To achieve the best performance, the waveguide photodetector was designed 1.5 μm wide and deeply etched through the film layer to minimize the capacitance. The calculated series resistances[7] are 105 Ω (40 Ω) respectively for 30 μm (80 μm) long photodetector. By assuming the parasitic capacitance of the bond-pad to be 12 fF[7], the calculated RC bandwidth is about 72 GHz (52 GHz). Therefore, the total bandwidth is about 38 GHz (32 GHz) for 30 μm (80 μm) long photodetector, mainly limited by the transit time bandwidth.

The active-passive epitaxial material was grown on a semi-insulating InP substrate by a three-step low pressure metal-organic-vapor-phase epitaxy (MOVPE)[8]. In the active part, a 120 nm thick absorption/active InGaAsP layer (Q1.55, $\lambda_{\text{gap}} = 1.55 \mu\text{m}$), embedded between two 190 nm quaternary confinement layers (Q1.25), covered by a 200 nm thick p-InP layer. In the passive part, the film layer (Q1.25) thickness is 500 nm, and n-doped ($N_d = 6 \times 10^{16} \text{cm}^{-3}$), covered by 200 nm thick n-InP layer with same doping level. The common layers for both active and passive part is 1300 nm gradually p-doped InP and 300 nm highly p-doped contact layer InGaAs. All the waveguides were fabricated by RIE. The access waveguide was shallowly etched to minimize the optical transmission loss, and the photodetector was deeply etched and stopped at $1 \times 10^{18} \text{cm}^{-3}$ n-InP layer below the film. The etching depth of the photodetector is about 3 μm . Polyimide was spun for passivation and planarization. Before metallisation, firstly we etched back the polyimide in the barrel etcher to expose p-InGaAs. Afterwards, we used the photoresist as a mask to protect the exposed p-contact, and etching the polyimide directionally to open n-InP contact layer. To form the metal contact, Ti/Pt/Au were evaporated on the top p-InGaAs and the lateral grounds (n-InP) through lift-off. Due to the limitation in the lift-off, the gap distance between the p- and n-contact was designed 10 μm . To minimize the RF transmission loss, the fabrication proceeded with the electroplating until the thickness of the gold is about 1.5 μm , which is three times larger than the skin depth[4]. The crosssection and the top view of the finished device are shown in figure 2. The photograph shows the photodetector with its coplanar waveguide transmission line, which are tapered

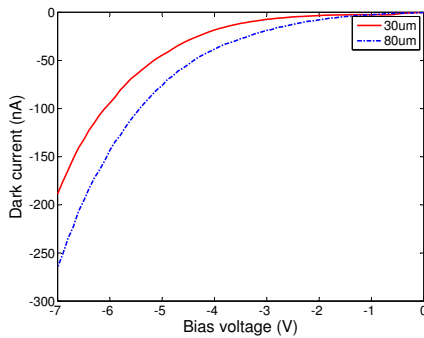


Figure 3: Measured dark current for $1.4\ \mu\text{m}$ wide deeply etched $30\ \mu\text{m}$ long (solid) and $80\ \mu\text{m}$ long (dash) photodetectors.

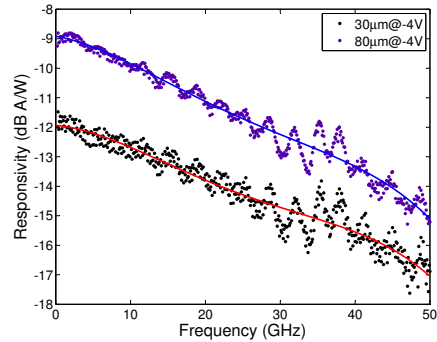


Figure 4: Frequency response of a $30\ \mu\text{m}$ long photodetector (below) and an $80\ \mu\text{m}$ long photodetector. The dot line is the measured data, and the the solid line is the fitting.

from the photodetector to the probepad which has a $100\ \mu\text{m}$ pitch. The central metal is $70\ \mu\text{m}$ wide, and the gap width is $30\ \mu\text{m}$.

Experimental results

The optical signal is coupled into the waveguide via the cleaved facet of the chip. All measurements were performed using on-wafer probing technique. The photodetectors exhibit low dark current, less than $50\ \text{nA}$ dark currents at $-4\ \text{V}$ bias voltage for the photodetectors up to $80\ \mu\text{m}$ long, figure 3.

On-wafer S-parameter measurements are performed in the range of $10\ \text{MHz}$ to $67\ \text{GHz}$ with a lightwave component analyzer and a $50\ \text{GHz}$ RF-probe. The photodetector was biased at $-4\ \text{V}$ through a $67\ \text{GHz}$ bias tee, and the injected wavelength from the lightwave analyzer is $1.55\ \mu\text{m}$ with $-1\ \text{dBm}$ optical power. The measured small signal frequency response is given in figure 4. The $30\ \mu\text{m}$ long photodetector achieved $35\ \text{GHz}$ 3-dB bandwidth, while the $80\ \mu\text{m}$ long photodetector obtained $28\ \text{GHz}$ bandwidth. The measured external reponsivity in the left axis showed that the external responsivity is $0.25\ \text{A/W}$ and $0.35\ \text{A/W}$ for $30\ \mu\text{m}$ and $80\ \mu\text{m}$ long photodetector, respectively. The measured RC bandwidth from S_{22} is in agreement with the calculated RC bandwidth. The measured total bandwidths are slightly smaller than the calculated bandwidth mainly because the depletion layer thickness is actually thicker than $500\ \text{nm}$ under $-4\ \text{V}$ reverse bias voltage, which further decreased the transit time bandwidth. Furthermore, the actual series resistance extracted from S_{22} is about $125\ \Omega$ ($60\ \Omega$) for $30\ \mu\text{m}$ ($80\ \mu\text{m}$) long photodetector, higher than the calculated value, which is due to the fabrication and the series resistance of the transmission line and the bondpad.

Conclusions

We demonstrated high-frequency waveguide photodetectors in an amplifier layer stack operating up to 35 GHz with 0.25 A/W external responsivity. This result enables the monolithic integration of source and high performance photodetector based on flexible butt-joint active-passive material without the need for a dedicated detector layer stack.

This work is partly funded by the Dutch National Broadband Photonics Access project and the Dutch National Smartmix project Memphis.

References

- [1] M. Kato, R. Nagarajan, J. Pleumeekers, P. Evans, A. Chen, A. Mathur, A. Dentai, S. Hurtt, D. Lambert, P. Chavarkar, M. Missey, J. Bäck, R. Muthiah, S. Murthy, R. Salvatore, C. Joyner, J. Rossi, R. Schneider, M. Ziari, F. Kish, and D. Welch, "40-channel transmitter and receiver photonic integrated circuits operating at per channel data rate 12.5 Gbit/s," *Electron. Lett.*, vol. 43, no. 8, Apr. 2007.
- [2] K. Kato, "Ultrawide-band/high-frequency photodetectors," *IEEE Transactions on Microwave Theory and Techniques*, vol. 47, no. 7, pp. 1265–1281, July 1999.
- [3] K. Kato, A. Kozen, Y. Muramoto, Y. Itaya, T. Nagatsuma, and M. Yaita, "110-GHz, 50%-efficiency mushroom-mesa waveguide p-i-n photodiode for 1.55- μ m wavelength," *IEEE Photon. Technol. Lett.*, vol. 6, no. 6, pp. 719–721, June 1994.
- [4] J. den Besten, "Integration of multiwavelength lasers with fast electro-optical modulators," Ph.D. dissertation, Technische Universiteit Eindhoven, Eindhoven, The Netherlands, 2004, ISBN 90-386-1643-0.
- [5] R. Sabella and S. Merli, "Analysis of InGaAs P-I-N photodiode frequency response," *IEEE J. Quantum Electron.*, vol. 29, no. 3, pp. 906–916, Mar. 1993.
- [6] K. Kato, S. Hata, K. Kawano, and A. Kozen, "Design of ultrawide-band, high-sensitivity p-i-n photodetectors," *IEICE Trans. Electron.*, no. 2, pp. 214–221, Feb. 1993.
- [7] Y.-G. Wey, K. Giboney, J. Bowers, M. Rodwell, P. Silvestre, P. Thiagarajan, and G. Robinson, "110-GHz GaInAs/InP double heterostructure p-i-n photodetectors," *J. Lightwave Technol.*, vol. 13, no. 7, pp. 1490–1499, July 1995.
- [8] Y. Barbarin, E. Bente, C. Marquet, E. Leclère, T. de Vries, P. van Veldhoven, Y. Oei, R. Nötzel, M. Smit, and J. Binsma, "Butt-joint reflectivity and loss in InGaAsP/InP waveguides," in *Proc. 12th Eur. Conf. on Int. Opt. (ECIO '05)*. Grenoble, France, April 6–8 2005, pp. 406–409.